

Doc-Start

Genome analysis

Core-genome scaffold comparison reveals the prevalence that inversion events are associated with pairs of inverted repeats

Dan Wang¹, Shuaicheng Li¹, Fei Guo³ and Lusheng Wang^{1,2,*}

¹Department of Computer Science, City University of Hong Kong, 83 Tat Chee Ave., Hong Kong

²University of Hong Kong Shenzhen Research Institute, Shenzhen Hi-Tech Industrial Park, Nanshan District, Shenzhen, PR China

³School of Computer Science and Technology, Tianjin University, Tianjin, PR China

*To whom correspondence should be addressed. E-mail: cswangl@cityu.edu.hk

Associate Editor: XXXXXXX

Received on XXXXX; revised on XXXXX; accepted on XXXXX

Abstract

Motivation: Genome rearrangement plays an important role in evolutionary biology and has profound impacts on phenotype in organisms ranging from microbes to humans. The mechanisms for genome rearrangement events remain unclear. Lots of comparisons have been conducted among different species. To reveal the mechanisms for rearrangement events, comparison of different individuals/strains within the same species (pan-genomes) is more helpful since they are much closer to each other.

Results: We study the mechanism for inversion events via core-genome scaffold comparison of different strains within the same species. We focus on two kinds of bacteria, *Pseudomonas aeruginosa* and *Escherichia coli*, and investigate the inversion events among different strains of the same species. We find an interesting phenomenon that long (larger than 10,000 bp) inversion regions are flanked by a pair of Inverted Repeats (IRs) (with lengths ranging from 385 bp to 27476 bp) which are often Insertion Sequences (ISs). This mechanism can also explain why the breakpoint reuses for inversion events happen. We study the prevalence of the phenomenon and find that it is a major mechanism for inversions. The other observation is that for different rearrangement events such as transposition and inverted block interchange, the two ends of the swapped regions are also associated with repeats so that after the rearrangement operations the two ends of the swapped regions remain unchanged. To our knowledge, this is the first time such a phenomenon is reported for transposition event.

Availability and Implementation: Source codes and examples for our methods are available at <https://drive.google.com/open?id=0B6GLgofcAnevc2hOZEJPyNnIEtg>

Contact: cswangl@cityu.edu.hk

Supplementary information: Supplemental tables are available at <https://drive.google.com/open?id=0B6GLgofcAnevc2hOZEJPyNnIEtg>.

1 Introduction

Comparative genomics studies show that genome rearrangement events often occur between two genomes. Genome rearrangement events play important role in speciation. The rearrangement operations include deletions, insertions, inversion, transposition, block interchange, translocation, fission and fusion, *etc.* The mechanisms for those

rearrangement events are still unclear. Here we study the mechanism for inversion events via core-genome scaffold comparison of different strains within the same species.

By comparing two genomes, we can find candidate rearrangement operations. However, the set of rearrangement operations to transform one genome into the other is not unique in many cases. Computing the rearrangement operations between two genomes under different assumptions is an active area, where intensive research have been conducted (Li *et al.*, 2006). It is reported that breakpoints appear more

often in repeated regions (Lemaitre *et al.*, 2009; Longo *et al.*, 2009). A summary of the where and wherefore of evolutionary breakpoints is given by Sankoff (2009). The prevalence of short inversions has been studied (Lefebvre *et al.*, 2003). Pevzner and Tesler found extensive breakpoint reuse for inversion events in mammalian evolution when comparing human and mouse genomic sequences (Pevzner and Tesler, 2003a,c).

An interesting problem is to reveal the mechanisms under the rearrangement operations. Many hypothetical mechanisms for the rearrangement operations have been reported (Gray, 2000). For example, Chen (2011) discussed mutational mechanisms for genomic rearrangements. To reveal the mechanisms under the rearrangement operations, comparison of different individuals/strains within the same species (pan-genomes) can be more helpful since strains within the same species are conserved.

A pan-genome, or supra-genome, describes the full complement of genes in a clade (typically for species in bacteria and archaea), which can have large variation in gene content among closely related strains. Pan-genomes were first studied by Tettelin more than a decade ago (Tettelin *et al.*, 2005). Several tools have been developed for pan-genome analysis. For example, GET_HOMOLOGUES (Contreras-Moreira and Vinuesa, 2013) is a customizable and detailed pan-genome analysis platform. BLAST atlas (Jacobsen *et al.*, 2011) visualizes which genes from the reference genome are present in other genomes. Mugsy-Annotator (Angiuoli *et al.*, 2011) identifies syntenic orthologs and evaluates annotation quality using multiple whole genome alignments. Characterization of the core and accessory genomes of *Pseudomonas aeruginosa* has been done by Ozer *et al.* (2014). For pan-genome analysis, genomes from different strains of the same species are decomposed to core blocks (in all the strains), dispensable blocks (in two or more strains) and strain-specific blocks (in one strain only). Here we extend the pan-genome analysis by comparing the core-genome scaffolds of different strains of the same species.

We study two types of bacteria, *Pseudomonas aeruginosa* and *Escherichia coli*, and investigate the inversion events among different strains of the same species. We find an interesting phenomenon that long (larger than 10,000 bp) inversion regions are flanked by pairs of Inverted Repeats (IRs) which are often Insertion Sequences (ISs). This mechanism also explains why the breakpoint reuses for inversion events happen. We study the prevalence of the phenomenon and find that it is a major mechanism for inversions. The other observation is that for different rearrangement events such as transposition and inverted block interchange, the two ends of the swapped regions are also associated with repeats so that after the rearrangement operations the two ends of the swapped regions remain unchanged. To our knowledge, this is the first time such a phenomenon is reported for transposition event.

2 Methods

We develop a pipeline to generate the core-genome blocks, dispensable blocks and strain-specific blocks based on the multiple sequence alignment produced by Mugsy (Angiuoli and Salzberg (2011)).

We then develop a computer program to generate the scaffolds of the strains from the core-genome blocks by repeatedly merging two consecutive blocks appearing in all the strains of the same species. In this way, the number of distinct blocks in the core-genome scaffold is reduced dramatically. For example, for *Pseudomonas aeruginosa*, before merging, there are 185 blocks in the core genome of the 25 strains. After merging, the scaffolds contain 69 blocks.

After that, we compute the inversion distance between two scaffolds. Computing the inversion distance between two scaffolds is a very hard and complicated combinatorial problem. Several algorithms have been

developed. Due to the difficulty of algorithm design, most of the algorithms only consider inversion events. However, a transposition/block-interchange event can be represented as 3 inversion events, and an inverted transposition/block-interchange event can be represented as 2 inversion events. Therefore, some of the computed inversion events may not be real. There are algorithms dealing with inversion and other rearrangement events such as block interchanges simultaneously. However, the weights for different events are different (again due to the difficulty of algorithm design). Thus, those algorithms still suffer from the problem of outputting inversions that are not real.

Our strategy here is to eliminate some obvious transposition, inverted transposition, block interchange, and inverted block interchange events.

For simplicity, we always assume that $G_1 = +1 + 2 \dots + n$ is the first input scaffold and $G_2 = \pi_1 \pi_2 \dots \pi_n$ is a sign permutation of the n blocks over the set $N = \{1, 2, \dots, n\}$ of n distinct blocks, where each integer $i \in N$ appear once in G_2 in the form of either $+i$ or $-i$. All the rearrangement operations are on G_2 .

A *transposition* swaps the order of two consecutive blocks/regions without changing their signs. A transposition (i, j, k) on regions π_i, \dots, π_{j-1} and $\pi_j \dots \pi_{k-1}$ transforms the sign permutation

$$\pi_1 \dots \pi_{i-1} \pi_i \dots \pi_{j-1} \pi_j \dots \pi_{k-1} \pi_k \dots \pi_n$$

into

$$\pi_1 \dots \pi_{i-1} \pi_j \dots \pi_{k-1} \pi_i \dots \pi_{j-1} \pi_k \dots \pi_n.$$

A transposition is *independent* if it transforms the sign permutation

$$\pi_1 \dots \pi_{i-2} \pi_{i-1} \pi_{i+1} \pi_i \pi_{i+2} \pi_{i+3} \dots \pi_n$$

into

$$\pi_1 \dots \pi_{i-2} \pi_{i-1} \pi_i \pi_{i+1} \pi_{i+2} \pi_{i+3} \dots \pi_n,$$

where $\pi_{i-1} \pi_i \pi_{i+1} \pi_{i+2}$ is either $+(q-1)+q+(q+1)+(q+2)$ or $-(q+2)-(q+1)-q-(q-1)$ for $\{q-1, q, q+1, q+2\} \subseteq N = \{1, 2, \dots, n\}$. Though an independent transposition swaps two consecutive blocks π_{i+1} and π_i instead of two regions π_i, \dots, π_{j-1} and $\pi_j \dots \pi_{k-1}$ as in the definition of a general transposition, a pre-process allows us to merge two consecutive blocks if they are consecutive in both input genomes. Thus, we can still handle some cases for swapping two consecutive regions. For example, the genome $+1 + 2 + 6 + 7 + 3 + 4 + 5 + 8$ becomes $+1 + 2 + 4 + 3 + 5$ after merging $+6 + 7$ (represented as $+4$) and $+3 + 4 + 5$ (represented as $+3$) and re-number $+8$ as $+5$ in the new representation. An independent transposition can change $+1 + 2 + 4 + 3 + 5$ into $+1 + 2 + 3 + 4 + 5$. In terms of breakpoint graph, the two blocks $\pi_{i+1} \pi_i$ in an independent transposition is involved in a 6-edge cycle and after the transformation the 6-edge cycle becomes three 2-edge cycles. In other words, the three breakpoints involved in the 6-edge cycle disappear after the transformation. See Figure 1.

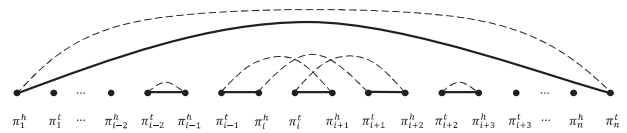


Fig. 1. The breakpoint graph for an independent transposition.

An *inverted transposition* swaps the order of two consecutive blocks/regions with one of the block's sign changed. An inverted transposition (i, j, k) on regions π_i, \dots, π_{j-1} and $\pi_j \dots \pi_{k-1}$ transforms the sign permutation $\pi_1 \dots \pi_{i-1} \pi_i \dots \pi_{j-1} \pi_j \dots \pi_{k-1} \pi_k \dots \pi_n$ into $\pi_1 \dots \pi_{i-1} -\pi_{k-1} \dots -\pi_j \pi_i \dots \pi_{j-1} \pi_k \dots \pi_n$ or $\pi_1 \dots \pi_{i-1} \pi_j \dots \pi_{k-1} -\pi_{j-1} \dots -\pi_i \pi_k \dots \pi_n$.

An inverted transposition is *independent* if it transforms the sign permutation $\pi_1 \dots \pi_{i-2} \pi_{i-1} -\pi_{i+1} \pi_i \pi_{i+2} \pi_{i+3} \dots \pi_n$

or

$\pi_1 \dots \pi_{i-2} \pi_{i-1} \pi_{i+1} \dots \pi_i \pi_{i+2} \pi_{i+3} \dots \pi_n$
 into
 $\pi_1 \dots \pi_{i-2} \pi_{i-1} \pi_i \pi_{i+1} \pi_{i+2} \pi_{i+3} \dots \pi_n$,
 where $\pi_{i-1} \pi_i \pi_{i+1} \pi_{i+2}$ is either $+(q-1) + q + (q+1) + (q+2)$ or $-(q+2) - (q+1) - q - (q-1)$ for $\{q_1, q, q+1, q+2\} \subseteq N = \{1, 2, \dots, n\}$.
 A block interchange swaps the locations of two separated blocks without changing their signs. A block interchange (i, j, k, l) on regions $\pi_i \dots \pi_j$ and $\pi_k \dots \pi_l$ transforms
 $\pi_1 \dots \pi_{i-1} \pi_k \dots \pi_l \pi_{j+1} \dots \pi_{k-1} \pi_i \dots \pi_j \pi_{l+1} \dots \pi_n$
 into
 $\pi_1 \dots \pi_{i-1} \pi_i \dots \pi_j \pi_{j+1} \dots \pi_{k-1} \pi_k \dots \pi_l \pi_{l+1} \dots \pi_n$.
 A block interchange is *independent* if it transforms the sign permutation $\pi_1 \dots \pi_{i-1} \pi_k \pi_{i+1} \dots \pi_{k-1} \pi_i \pi_{k+1} \dots \pi_n$
 into
 $\pi_1 \dots \pi_{i-1} \pi_i \pi_{i+1} \dots \pi_{k-1} \pi_k \pi_{k+1} \dots \pi_n$,
 where $\pi_{i-1} \pi_i \pi_{i+1}$ is either $+q + (q+1) + (q+2)$ or $-(q+2) - (q+1) - q$ and $\pi_{k-1} \pi_k \pi_{k+1}$ is either $+p + (p+1) + (p+2)$ or $-(p+2) - (p+1) - p$ for $\{q, q+1, q+2\} \subseteq N$ and $\{p, p+1, p+2\} \subseteq N$. Similarly, the two blocks π_k and π_i are involved in two (interleaving) 4-edge cycles in the breakpoint graph and after the transformation, they become four 2-edge cycles. In other words, there are four breakpoints at the two ends of the two blocks, after the transformation, the four breakpoints disappear. See Figure 2. 1.

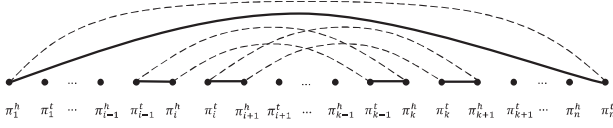


Fig. 2. The breakpoint graph for an independent block interchange.

An *inverted block interchange* swaps the location of two separated blocks with both signs of the two blocks changed. An inverted block interchange (i, j, k, l) on regions $\pi_i \dots \pi_j$ and $\pi_k \dots \pi_l$ transforms
 $\pi_1 \dots \pi_{i-1} \pi_i \dots \pi_j \pi_{j+1} \dots \pi_{k-1} \pi_k \dots \pi_l \pi_{l+1} \dots \pi_n$
 into
 $\pi_1 \dots \pi_{i-1} \pi_i \dots \pi_j \pi_{j+1} \dots \pi_{k-1} \pi_k \dots \pi_l \pi_{l+1} \dots \pi_n$.

An inverted block interchange is *independent* if it transforms the sign permutation $\pi_1 \dots \pi_{i-1} \pi_i \dots \pi_j \pi_{j+1} \dots \pi_{k-1} \pi_k \dots \pi_l \pi_{l+1} \dots \pi_n$
 into $\pi_1 \dots \pi_{i-1} \pi_i \pi_{i+1} \dots \pi_{k-1} \pi_k \pi_{k+1} \dots \pi_n$,
 where $\pi_{i-1} \pi_i \pi_{i+1}$ is either $+q + (q+1) + (q+2)$ or $-(q+2) - (q+1) - q$ and $\pi_{k-1} \pi_k \pi_{k+1}$ is either $+p + (p+1) + (p+2)$ or $-(p+2) - (p+1) - p$ for $\{q, q+1, q+2\} \subseteq N$ and $\{p, p+1, p+2\} \subseteq N$. Again, there are four breakpoints at the two ends of the two blocks $-\pi_i$ and $-\pi_k$, after the transformation, the four breakpoints disappear.

After eliminating independent transposition, inverted transposition, block interchange and inverted block interchange events, we use GRIMM-Synten (Tesler, 2002a,b) to compute the inversion distance between pairwise core-genome scaffolds. We only seriously consider the cases where the rearrangement distance is small. When the rearrangement distance is large, there may be multiple solutions for the inversion history. Thus, in this case, the computed inversion events may not be real.

Finally, we developed a pipeline to compare sequences at the two ends of each inversion region to see whether a pair of inverted repeats exists. Once the inverted repeats are found, the pipeline can also search all the strains and mark down its positions in different strains.

3 Results

3.1 *Pseudomonas aeruginosa*

Complete genome sequences of 25 *Pseudomonas aeruginosa* strains PACS2 (AAQW01000001.1), NCGM1984 (AP014646.1), NCGM1900 (AP014622.1), NCGM2.S1 (AP012280.1), Carb01_63 (CP011317.1), SCV20265 (CP006931.1), UCBPP-PA14 (CP000438.1), VRFPA04 (CP008739.2), DSM_50071 (CP012001.1), 19BR (AFXJ01000001.1), 213BR (AFXK01000001.1), B136-33 (CP004061.1), PA7 (CP000744.1), LES431 (CP006937.1), PA1 (CP004054.2), YL84 (CP007147.1), LESB58 (FM209186.1), M18 (CP002496.1), RP73 (CP006245.1), DK2 (CP003149.1), MTB1 (CP006853.1), PAO1 (AE004091.2), F22031 (CP007399.1), PA1R (CP004055.1), and FRD1 (CP010555.1) were downloaded from NCBI GenBank. The details of these 25 *Pseudomonas aeruginosa* strains are listed in Supplemental Table S1. The genome lengths of these strains are between 6.2 mbp (million base pair) and 7.5 mbp. We used our pipeline to compute the core-genomes and obtained 533 core-blocks with lengths ranging from 58 bp to 83 kbp (kilo base pair) and total lengths ranging from 5.33 mbp to 5.6 mbp (million base pair) which account for 74.8% - 88.2% of the strains' genomes. We then eliminated core blocks with length less than 500 bp and iteratively merged core blocks that were consecutive for all the 25 strains. As a result, 69 (merged) blocks were obtained and the 25 strains led to 8 different scaffolds as shown in Figure 3. The scaffold for each *Pseudomonas aeruginosa* strain is in Supplemental Table S4. For any pair of consecutive blocks in one group, there must be a different group in which there is a breakpoint between the two blocks when comparing the two scaffolds.

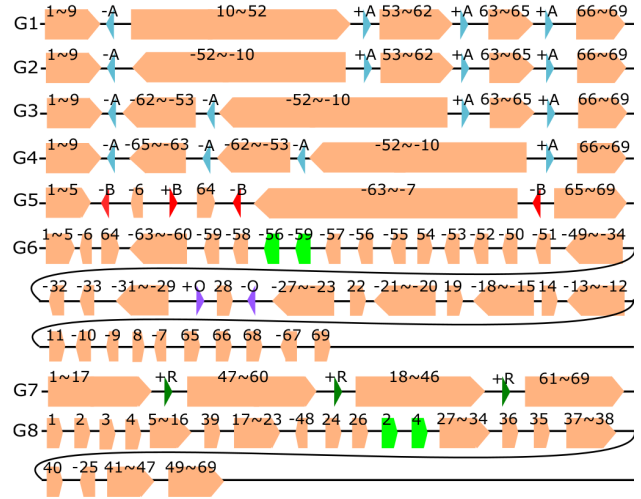


Fig. 3. Eight groups of scaffolds for the 25 *Pseudomonas aeruginosa* strains. Each orange block stands for a merged block which may represent several consecutive core-genome blocks. The numbers above each orange block indicate the included core-genome blocks, for example, 1~5 means the orange block includes five core-genome blocks, which are Blocks 1, 2, 3, 4 and 5. Repeats A, B, O are represented by blue, red and purple triangles respectively. The arrow directions indicate positive/negative strand.

Group 1 contains 13 strains, which are *Pseudomonas aeruginosa* strains NCGM1984, B136-33, YL84, LESB58, M18, SCV20265, LES431, UCBPP-PA14, DK2, MTB-1, DSM_50071, Carb01_63, and F22031. Group 2 contains 6 strains, which are strains RP73, 213BR, PA1, PA1R, 19BR, and PAO1. Groups 3-8 contain 1 strain each and the respective strains are PACS2, FRD1, NCGM2.S1, VRFPA04, NCGM1900, and PA7.

We computed the pairwise inversion distance between scaffolds after eliminating other kinds of independent rearrangement events such as transpositions, inverted-transpositions, block-interchanges, and inverted-block-interchanges. For each of the 8 scaffolds, we chose a scaffold with the minimum inversion distance (after eliminating other independent rearrangement events) to compare. The purpose was to compare two scaffolds with a small number of inversions so that we can observed real inversions between them. From Table 1, it can be seen that Group 1 is the closest group to all the other groups except for Group 6. The closest group to Group 6 is Group 5, where the inversion distance is 7. In total,

Table 1. Shortest inversion distance for each of the 8 groups of *Pseudomonas aeruginosa*.

sG^a	cG^a	Inv_d^b	$inversion^c$	l^d	IR^e	R_d^b
1	2	1	(10,52)	4.061	A(2)	0
2	1	1	(-52,-10)	4.061	A(2)	0
3	1	1	(-62,-10)	4.769	A(2)	0
4	1	1	(-65,-10)	5.699	A(2)	0
5	1	3	(-6,-6)	0.0597	B(0)	0
			(64,64)	0.0068	B(0)	
			(-64,-7)	5.879	B(0)	
6	5	7	(28,28)	0.0130	O(0)	3
			(54,54)	0.0025	None	
			(22,22)	0.0032	None	
			(19,19)	0.0031	None	
			(14,14)	0.0021	None	
			(11,11)	0.0054	None	
			(8,8)	0.0074	None	
7	1	0	None	N/A	N/A	1
8	1	0	None	N/A	N/A	4

^aColumn sG is the source scaffold group, Column cG is the closest scaffold group.

^b Inv_d indicates the inversion distance between sG and cG after eliminating other independent rearrangement events. R_d indicates the distance of other independent rearrangement events.

^cThe two numbers indicate the starting and ending block of the inversion in the source scaffold (sG). Rearrangement scenario is calculated from the source group to the closest group

^d l is the length (in Mbp) of inversion of the core-genome segments.

^eColumn IR lists which pair of inverted repeats (A, B or O) flanks the inversion. The numeric code: 0 indicates the respective IR was found only in the source group, 1 indicates the IR was found only in the closest group, 2 indicates the IR was found in both groups.

there are 13 inversion events among the 7 distinct pairs of scaffolds (Table 1, where pair 1 and 2 appears twice). Among the 13 inversion regions, 7 of them are flanked by a pair of IRs. The remaining 6 inversions with no IRs found at the two ends of the inversion regions are very short and their lengths are from 2100 bp to 7400 bp. For each of the first three (Table 1, rows 1-4) inversions, the lengths of the inversion regions are more than 4 mbp, and we find a pair of IRs (+A/-A) at the two ends of each of the three long inversion regions. For the pair of Groups 5 and 1, there are three inversions and the lengths of the three inversions in the core-genome are 5.879 mbp, 0.597 mbp, and 6.8 kbp, respectively. Interestingly, we find a repeat B that appears four times in Both Scaffold 1 and Scaffold 5, where B appear as $-B$ once and as $+B$ three times in Scaffold 1. The four occurrences of B form a pair of IRs at the two ends of each of the 3 inversion regions (See Figure 3). For Groups 6 and 5, there exist two independent transpositions and one inverted transposition (See supplement-1). After eliminating the three independent rearrangement events, there are 7 inversions between Groups 6 and 5 which are calculated by GRIMM-Synteny (See Supplement-1) and only one inversion (28,28)

is flanked by a pair of IRs (See Table 1). Note that both -56 and -59 appear twice in Scaffold 6. We remove the green blocks in Figure 3 in our comparison. Among these seven inversions, only one inversion (28,28) is longer than 10000bp and flanked by a pair of IRs (+O/-O). Group 1 can be obtained from Group 7 with one independent transposition. A repeat $+R$ appears three times at the ends of the two blocks involved in the transposition. See Figure 3). Those occurrences of $+R$ play an important role in the transposition and the details will be discussed in Section 2.1.2. For Group 8 and 1, there exist two independent transpositions and two independent inverted transpositions (See Supplement-1). After eliminating the four independent rearrangement events, the scaffolds for Group 8 and 1 are actually the same and the inversion distance between them is zero. Again, both Blocks 2 and Block 4 appear twice in Group 8. (The physical positions of all the copies of Blocks 2 and 4 in Group 8 are in Supplemental Table S5h). We remove the green blocks in Figure 3 in our comparison.

For the first inversion between Group 1 and 2, there are 13 strains in Group 1 and 6 strains in Group 2. All the strains in Group 1 and Group 2 contain Repeat $+A$ and $-A$ as shown in Figure 3. The physical positions as well as the lengths of the repeats differ slightly in different strains. See Supplemental Table S5a. Thus, the inversion (from Blocks 10 to 52) between Scaffold 1 and Scaffold 2 (row 1 in Table 1) is found between the 13×6 pairs of strains in these two groups. For the remaining inversions listed in Table 1, the physical positions, the lengths of repeats and core-genome blocks (at the two ends of an inversion) in different strains are given in Supplemental Tables S5b-e.

In summary, three different pairs of IRs are found and we use $+A/-A$, $+B/-B$ and $+O/-O$ to differentiate these three pairs. We also find three copies of $+R$ in comparison of Groups 1 and 7. The locations of these repeats in the scaffolds are shown in Figure 3. The lengths (in bp), gene products and protein IDs (in NCBI Protein database) of these repeats are listed in Supplemental Table S9.

3.1.1 Breakpoint reuse

The three inversion steps from Scaffold 1 to 5 are shown in Figure 4, where it can be seen that there is a $+B$ and three $-Bs$ in Scaffold 5. The three inversion events are $-B-6+B$ to $-B6+B$, $+B7-64-B$ to $+B-64-7-B$ and $+B-64-B$ to $+B64-B$ and the breakpoint the black arrow points at in Figure 4 is used three times.

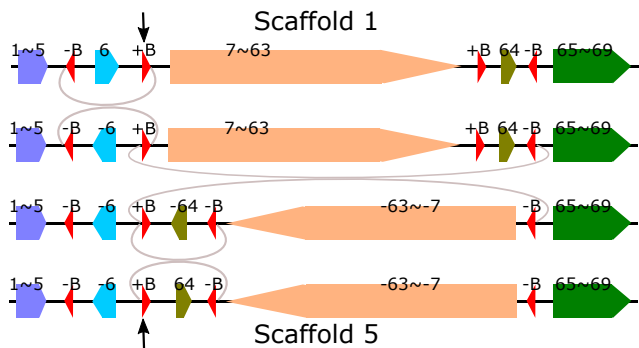


Fig. 4. Three inversion steps from scaffold 1 to scaffold 5. The breakpoint between -6 and 64 in Scaffold 5 is used three times. See the black arrow.

Here $+B$ plays a crucial role in the three inversions and is used three times, each time $+B$ and $-B$ form a pair of inverted repeats at the two ends of the inversion regions. Now let us have a close look at $+B$ (of length 820 bp), we can see that for the first inversion ($-B-6+B$ to $-B6+B$), the real cutting points (breakpoints) are at the left end of $-B$ and the right end of $+B$, while for the other two inversions ($+B7-64-B$ to $+B-64-7-B$ and

+B-64-B to +B+64-B), the real cutting points (breakpoints) are at the left end of +B and the right end of -B. Here the real cutting point does not seem to be important and the repetitive element B should be viewed as the breakpoint.

Another interesting finding is that for Groups 1, 2, 3 and 4, each scaffold contains a -A and three +As. (See Figure 3.) Theoretically, this -A can be reused three times with each of the three +As. However, we did not observe such three breakpoint reuses in a single pairwise scaffold comparison. But it has been observed that this -A, along with each of the three +As, mediate three different inversion events which occur between Group 1 and Group 2, Group 1 and Group 3, and Group 1 and Group 4, respectively (Table 1, row 2-4).

3.1.2 Transposition

Figure 5 gives the detailed scaffolds for Groups 1 and 7. Both Scaffolds 1 and 7 contain four merged core blocks (1~17), (18~46), (47~60), and (61~69). Moreover, both Scaffolds 1 and 7 contain another two non-core blocks DS1 and DS2, where the occurrences of DS1 and DS2 in both scaffolds are 100% identical. Besides, there are three occurrences of a repeat +R in both scaffolds. It can be seen that by swapping 47~60 and DS1 with 18~46 and DS2, Scaffold 7 is transferred into Scaffold 1. The most interesting finding is the three occurrences of +R located at the three breakpoints of the transposition. We believe that this three occurrences of +R play an important role in this transposition event because the repeat +R can make sure the two ends of the two swapped regions remain unchanged before and after the transposition. This is similar to the mechanism that inversion regions are flanked by a pair of IRs, where after the inversion the two ends of the inversion region remain the same. For reference, the physical positions of the three +Rs, DS1, DS2 and Blocks 47, 60, 18 and 46 in the chromosomes of Group 7 and 1 are listed in Supplemental Table S5f.

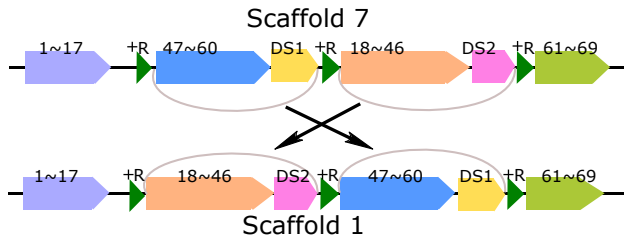


Fig. 5. Both Scaffolds 1 and 7 contain four merged core blocks (1~17), (18~46), (47~60), and (61~69). Moreover, both Scaffolds 1 and 7 contain another two non-core blocks DS1 and DS2, where the occurrences of DS1 and DS2 in both scaffolds are 100% identical. There are three occurrences of a repeat +R in both scaffolds.

3.2 *Escherichia coli*

We selected 31 *Escherichia coli* strains (identification number (id) 1 to 31) with complete sequences from 17 genome families at NCBI's GenBank. These 31 strains are SE15 (AP009378.1), IAI39 (CU928164.2), EC4115 (CP001164.1), CFT073 (AE014075.1), CE10 (CP003034.1), O103:H2 str. 12009 (AP010958.1), C227-11 (CP011331.1), 536 (CP000247.1), K-12 substr. MG1655 (U00096.3), ST2747 (CP007392.1), NA114 (CP002797.2), 042 (FN554766.1), O111:H- str. 11128 (AP010960.1), O145:H28 str. RM13514 (CP006027.1), O104:H4 str. 2011C-3493 (CP003289.1), SE11 (AP009240.1), SS52 (CP010304.1), APEC O78 (CP004009.1), SMS-3-5 (CP000970.1), DH1Ec095 (CP012125.1), 1303 (CP009166.1), O157:H7 str. Sakai (BA000007.2), 55989 (CU928145.2), B str. REL606 (CP000819.1), O83:H1 str. NRG 857C (CP001855.1), UMN026 (CU928163.2), PCN033 (CP006632.1), 789 (CP010315.1),

O127:H6 str. E2348/69 (FM180568.1), P12b (CP002291.1), and ED1a (CU928162.2). The detailed information of these 31 strains is listed in Supplemental Table S2. The genome lengths of these strains are between 4614223 bp and 5585613 bp. Our pipeline found 344 core blocks. The lengths of these core blocks range from 45 bp to 72931 bp and the total core-genome lengths in different strains range from 4006932 bp to 4246034 bp which account for 74.07%-88.42% of the strains' genomes. After eliminating core-blocks with length less than 500 bp and repeatedly merge two consecutive core-blocks (that are consecutive for all the 31 strains), we obtained 49 (merged) blocks and the 31 strains formed 9 groups of scaffolds (G1-G9 as shown in Figure 6). The scaffold for each of the 31 *Escherichia coli* strain is given in Supplemental Table S6.

Group 1 contains 21 strains which are *Escherichia coli* strains EC4115, CE10, C227-11, K-12 substr. MG1655, ST2747, 042 O104:H4 str. 2011C-3493, SE11, SS52, APEC O78, DH1Ec095, 1303, O157:H7 str. Sakai, 55989, B str. REL606, O83:H1 str. NRG 857C, UMN026, PCN033, 789, O127:H6 str. E2348/69, and ED1a. Group 2 contains 3 strains, SE15, CFT073 and 536. Groups 3-9 contain 1 strain each and the respective strains are O145:H28 str. RM13514, SMS-3-5, P12b, IAI39, O103:H2 str. 12009, NA114, and O111:H- str. 11128.

After computing pairwise inversion distance among the 9 scaffolds, we selected a scaffold with minimum inversion distance for each of the 9 scaffolds as shown in Table 2 for comparison. From Table 2, it can be seen that Group 1 is the closest group to all the other 8 groups with inversion distances ranging from 0 to 4. The closest group to Group 1 is Group 2, where the sign of Block 24 is different. In total, there are 17 inversion

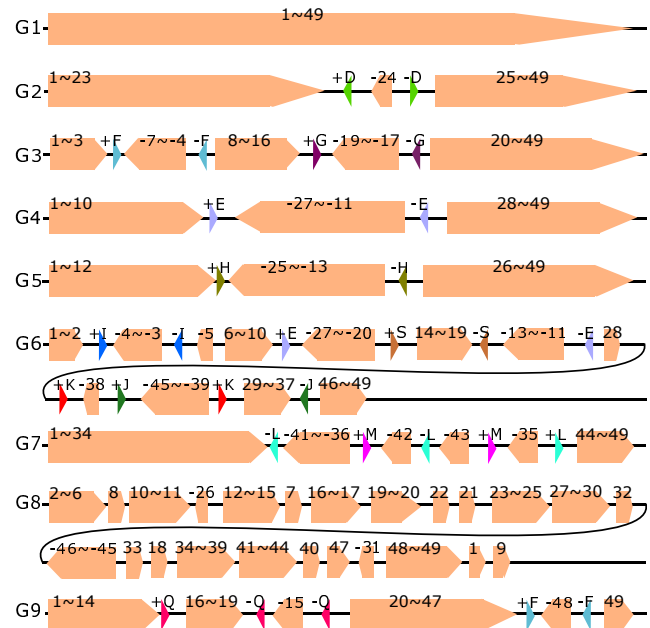


Fig. 6. Nine groups of scaffolds for the 31 *Escherichia coli* strains

events among the 8 distinct pairs in Table 2 (the pair of Group 1 and Group 2 appears twice) and the inversion region lengths varies from 0.0075 mbp to 1.402 mbp. (See Table 2.) Among the 17 inversion regions, 12 of them are found to be flanked by a pair of inverted repeats in the strains of the source groups. For inversion (-5,5) between Group 1 and Group 6 (row 6 in Table 2) and the four inversions between Group 1 and 8, no pairs of inverted repeats are found at the two ends of the block. The length of inversion (-5,5) (Row 6 in Table 2) is short (7.5 kbp). The four computed inversions between Group 1 and 8 may not be true since there are another 6

Table 2. Shortest inversion distance for each of the 9 groups of *Escherichia coli*.

<i>sG</i>	<i>cG</i>	<i>Inv_d</i>	<i>inversion</i>	<i>l</i>	<i>IR</i>	<i>R_d</i>
1	2	1	(24,24)	0.0041	D(1) ^a	0
2	1	1	(-24,-24)	0.0041	D(0) ^a	0
3	1	2	(-7,-4)	0.2763	F(0)	0
			(-19,-17)	0.1940	G(0) ^b	0
4	1	1	(-27,-11)	1.402	E(0)	0
5	1	1	(-25,-13)	1.111	H(0)	0
6	1	4	(-4,-3)	0.2706	I(0)	1
			(-5,-5)	0.0075	-	
			(-45,37)	1.4108	J(0)	
			(-38,-29)	1.2756 ^c	K(0)	
7	1	3	(-43,35)	0.0642	L(0)	0
			(-42,35)	0.1055 ^d	M(0)	
			(-41,-35)	0.3944 ^e	L(0)	
8	1	4	(See Supplement-1)	N/A	N/A	6
9	1	1	(48,48)	0.0651	F(0)	1

^aIn Group 1, only Strain SE15 has +D/-D at the ends of 24

^bIn Group 2, only Strain O157:H7 str. Sakai has +G/-G at the ends of (-19,-17)

^c*l*=length of Block 38 + length from Block 29 to Block 37 in Group 6.

^d*l*=length of Block 42 + length of Block 35 in Group 7.

^e*l*=length from Block 41 to Block 36 + length of Block 35 in Group 7.

other rearrangement events between the two scaffolds (Row 8 in Table 2). For Groups 6 and 1, the rearrangement distance is five (one independent inverted block interchange and a sequence of four inversions). See Table 2. At the breakpoints of this inverted block interchange, we also find IRs and we will discuss it in Section 2.2.2. For Group 8 and 1, after eliminating six independent transpositions, there exists a sequence of four inversions (See Supplement-1). Only one of these four inversions is flanked by a pair of IRs. We observe that there are seven copies of Block 45 in Group 8 and we used the -45 next to -46 for comparison. The distance between Group 1 and Group 8 is big (6 transpositions + 4 inversions) and thus our predicted rearrangement history between Group 1 and Group 8 may not be correct. (Again, for reference, the physical positions of these seven copies of Block 45 in the chromosome of Group 8 are in Supplemental Table S7i.) To obtain Group 1 from Group 9, an independent inverted transposition and an inversion (Block -48 in Scaffold 9) are required. (See Table 2). The inverted region (Block -48) is flanked by a pair of IRs (+F/-F) in the Group 9. (See Figure 6.) In addition, we find that this inverted transposition event is also associated with repeats and we will discuss this in Section 2.2.3.

For all the inversions listed in Table 2, the physical positions, the lengths of repeats and core-genome blocks (at the two ends of inversions) in different strains are given in Supplemental Table S7a-g.

We find a total of 12 different types of pairs of inverted repeats and use letters from +D/-D to +M/-M, +S/-S and +Q/-Q to label and differentiate these 12 pairs of IRs. The locations of these IRs in the scaffolds are shown in Figure 6. The lengths (in bp), gene products and protein IDs (in NCBI Protein database) of these 12 IRs are listed in Supplemental Table S8. We note that 7 of these 12 pairs of IRs contain genes which encode transposase.

3.2.1 Breakpoint reuse

The three inversion steps from Scaffolds 1 to 7 are illustrated in Figure 7. From Figure 7, it can be seen that The breakpoint between 41 and 42 in Scaffold 1 is used twice. The corresponding inversion regions are flanked by -L and +L.

It is worth pointing out that the two +Ms in Scaffold 1 form a pair of directed repeats (DRs). After inversion (35,-41), the pair of directed repeats (DRs) of M becomes a pair of inverted repeats. This means that a pair of DRs has the potential to mediate inversions.

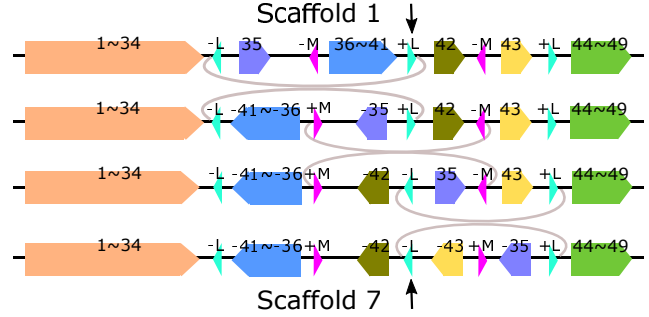


Fig. 7. Three inversions between Scaffolds 1 and 7. The breakpoint between 41 and 42 in Scaffold 1 is used twice. See the black arrow.

3.2.2 Inverted Block Interchange

We find an inverted block interchange between Scaffold 6 and 1 and we use Figure 8 to illustrate. In Figure 8, Region +E-27~-20+S and -S13~-11-E in Scaffold 6 are inversely interchanged with each other to obtained Scaffold 1. The existence of two pairs of IRs (+E/-E and +S/-S) makes sure the two ends of the swapped blocks remain unchanged after the inverted block interchange event. The physical positions of +E/-E, +S/-S and Blocks 27, 20, 13 and 11 in Groups 6 and 1 are listed in Supplemental Table S7h.

The other explanation is that an inverted block interchange can be replaced by two inversions. Figure 9 shows the two inversions which can replace the inverted block interchange of Blocks -27~-20 and Block -13~-11. Each of these two inversions is flanked by a pair of IRs (See Figure 9).

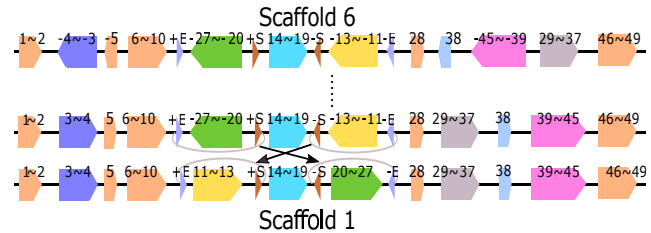


Fig. 8. Inverted block interchange of Region -27~-20 and Region -13~-11 between Scaffolds 6 and 1. +E/-E and +S/-S are two pairs of IRs. The steps from Scaffold 6 to the middle scaffold are omitted.

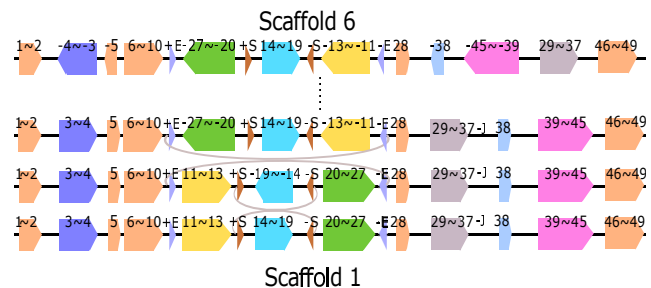


Fig. 9. Two inversions which can replace the inverted block interchange of Regions -27~-20 and -13~-11 between Scaffold 6 and 1. The first inversion is flanked by +E and -E and the second inversion is flanked by +S and -S. The steps from the Scaffold 6 to its next scaffold are omitted.

3.2.3 Inverted Transposition

Figure 10 shows the inverted transposition from Scaffolds 9 to 1: Block -15 and region 16~18 in Scaffold 9 are swapped with each other with the sign of Block -15 changed. Block -15 is flanked by a pair of directed repeats (DRs) (-Q,-Q) and Region 16~18 is flanked by a pair of IRs (+Q,-Q) in Scaffold 9. These three occurrences of Repeat Q can make the ends of Block -15 and Block 16-18 remain unchanged after the inverted transposition (with the sign of Block -15 changed). The physical positions of the three copies of Repeat Q and Blocks 15, 16 and 18 in the chromosomes of Group 9 and 1 are listed in Supplemental Table S7j.

The other explanation is that the inverted transposition can be replaced by two inversions: the first inversion is from Blocks 16 to -15 and the second inversion is from Blocks -19 to -16 (See Figure 11). Both of these two inversions are flanked by a pair of IRs (+Q/-Q).

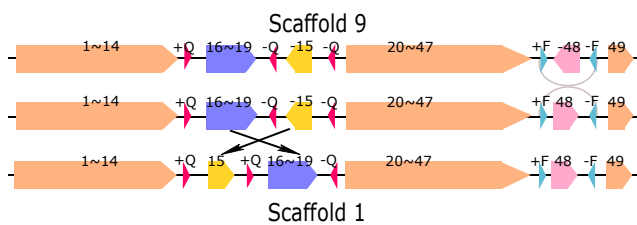


Fig. 10. Inverted transposition of Region 16~19 and Block 15 between Scaffold 9 and 1. There are three occurrences of Repeat Q with different signs. From Scaffold 9 to the next scaffold, there is an inversion of Block 48 which are flanked by +F and -F.

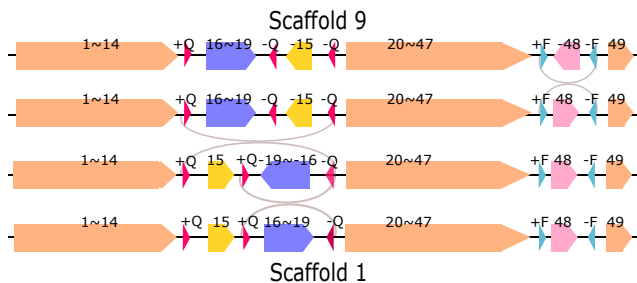


Fig. 11. Two inversions which can replace the inverted transposition of Region 16~19 and Block 15 between Scaffold 9 and 1. Both of the two inversions are flanked by a pair of IRs (+Q/-Q). From Scaffold 9 to the next scaffold, there is an inversion of Block 48 which are flanked by +F and -F.

4 Discussions

Breakpoint reuses for inversion event was first reported by Pevzner and Tesler (2003b) when comparing human and mouse genomic sequences. Their analysis shows that at least 245 rearrangements of 281 synteny blocks occurred between human and mouse genome. It is estimated that any human & mouse rearrangement scenario requires at least 190 breakpoint reuses (Pevzner and Tesler, 2003b). Their analysis on X chromosome between human and mouse illustrates that there are two different most parsimonious scenarios. Both contain three (different) breakpoint reuses. Sankoff and Trinh (2005) show that breakpoint reuse is very sensitive to the proportion of blocks excluded. Attie *et al.* (2011) also show that the inferred breakpoint reuse rate depends on synteny block resolution in human-mouse genome comparisons. Statistics analyzes showed that breakpoints are often associated with repetitive elements and the density

of breakpoints in small intergenes appears significantly higher than in gene deserts (Longo *et al.*, 2009; Sankoff, 2009). However, the mechanism for breakpoint reuse is not clear. Here our observation that long inversions are flanked by a pair of inverted repetitive elements can clearly explain why breakpoint reuse happens for inversions. The comparative results for the two different kinds of bacteria also illustrate the prevalence of this phenomenon. Recently, breakpoint reuse for inversions has been reported in *Drosophila* genus (Puerma *et al.*, 2014; Orengo *et al.*, 2015) as well as *Saccharomyces pastorianus* (Hewitt *et al.*, 2014). Rajaraman *et al.* (2013) suggested that rearrangements could be driven by the ISs and the positions of the inversion breakpoints in their study were also highly correlated with IS: 76 of the 118 mapped breakpoints were close (<1000 nt distant) to some predicted IS, whereas this number drops to 39 for uniformly sampled random coordinates (P-value <10⁻³). Darmon and Leach (2014) reviewed many examples of prokaryotic genomic rearrangements which were induced by natural transposable elements and pointed out that recombination between IRs can result in an inversion of the internal DNA sequence. The association between IR and genome rearrangement breakpoints was also reported in previous studies on mammals and drosophila genomes (Thomas *et al.*, 2011; Ranz *et al.*, 2007; Bailey *et al.*, 2004; Armengol *et al.*, 2003; Samonte and Eichler, 2002). Accounting for this phenomenon in order to reduce the space of optimal inversion scenarios was explored. Armengol *et al.* (2003) observed that nine primary regions involved in human genomic disorders which show changes in the order or the orientation of mouse/human synteny segments were often flanked by segmental duplications in the human sequence. They also found that 53% of all evolutionary rearrangement breakpoints associate with segmental duplications, as compared with 18% expected in a random location of breaks along the chromosome (P < 10⁻⁴). Ranz *et al.* (2007) analyzed the breakpoint regions of the 29 inversions that differentiate the chromosomes of *Drosophila melanogaster* and two closely related species, *D. simulans* and *D. yakuba*, and reconstructed the molecular events that underlie their origin. Experimental and computational analysis revealed that the breakpoint regions of 59% of the inversions (17/29) are associated with inverted duplications of genes or other non-repetitive sequences. They also for the first time reconstruct the reuse of a breakpoint region in Diptera (Ranz *et al.*, 2007).

Dataset

***Pseudomonas aeruginosa* data set.** On 10 June 2015, We downloaded all of the publicly available *Pseudomonas aeruginosa* complete genomes from GenBank at the NCBI. The detailed information of the 25 *Pseudomonas aeruginosa* strains is listed in Supplemental Table S1.

***Escherichia coli* data set.** At NCBI's GenBank, there are total 150 complete genomes and 33 genome groups. 21 genome groups have complete genomes for *Escherichia coli*. We downloaded complete genomes of 31 *Escherichia coli* strains from 17 different genome groups and the detailed information of our dataset is in Supplemental Table S2.

Funding

This work is supported by a National Science Foundation of China (NSFC 61373048) and a grant from the Research Grants Council of the Hong Kong Special Administrative Region, China (CityU 123013).

Conflict of Interest: none declared.

References

- Angiuoli, S. V. and Salzberg, S. L. (2011). Mugsy: fast multiple alignment of closely related whole genomes. *Bioinformatics*, **27**(3), 334–342.
- Angiuoli, S. V., Hotopp, J. C. D., Salzberg, S. L., and Tettelin, H. (2011). Improving pan-genome annotation using whole genome multiple alignment. *BMC bioinformatics*, **12**(1), 272.
- Armengol, L., Pujana, M. A., Cheung, J., Scherer, S. W., and Estivill, X. (2003). Enrichment of segmental duplications in regions of breaks of synteny between the human and mouse genomes suggest their involvement in evolutionary rearrangements. *Human molecular genetics*, **12**(17), 2201–2208.
- Attie, O., Darling, A. E., and Yancopoulos, S. (2011). The rise and fall of breakpoint reuse depending on genome resolution. *BMC bioinformatics*, **12**(Suppl 9), S1.
- Bailey, J. A., Baertsch, R., Kent, W. J., Haussler, D., and Eichler, E. E. (2004). Hotspots of mammalian chromosomal evolution. *Genome biology*, **5**(4), 1.
- Chen, J.-M. (2011). Genomic rearrangements: Mutational mechanisms. *eLS*.
- Contreras-Moreira, B. and Vinuesa, P. (2013). Get_homologues, a versatile software package for scalable and robust microbial pangenome analysis. *Applied and environmental microbiology*, **79**(24), 7696–7701.
- Darmon, E. and Leach, D. R. (2014). Bacterial genome instability. *Microbiology and Molecular Biology Reviews*, **78**(1), 1–39.
- Gray, Y. H. (2000). It takes two transposons to tango: transposable-element-mediated chromosomal rearrangements. *Trends in Genetics*, **16**(10), 461–468.
- Hewitt, S. K., Donaldson, I. J., Lovell, S. C., and Delneri, D. (2014). Sequencing and characterisation of rearrangements in three *S. pastorianus* strains reveals the presence of chimeric genes and gives evidence of breakpoint reuse. *PLoS One*, **9**(3), e92203.
- Jacobsen, A., Hendriksen, R. S., Aarestrup, F. M., Ussery, D. W., and Friis, C. (2011). The salmonella enterica pan-genome. *Microbial ecology*, **62**(3), 487–504.
- Lefebvre, J.-F., El-Mabrouk, N., Tillier, E., and Sankoff, D. (2003). Detection and validation of single gene inversions. *Bioinformatics*, **19**(suppl 1), i190–i196.
- Lemaitre, C., Zaghloul, L., Sagot, M.-F., Gautier, C., Arneodo, A., Tannier, E., and Audit, B. (2009). Analysis of fine-scale mammalian evolutionary breakpoints provides new insight into their relation to genome organisation. *BMC genomics*, **10**(1), 335.
- Li, Z., Wang, L., and Zhang, K. (2006). Algorithmic approaches for genome rearrangement: a review. *Systems, Man, and Cybernetics, Part C: Applications and Reviews, IEEE Transactions on*, **36**(5), 636–648.
- Longo, M. S., Carone, D. M., Green, E. D., O'Neill, M. J., O'Neill, R. J., et al. (2009). Distinct retroelement classes define evolutionary breakpoints demarcating sites of evolutionary novelty. *BMC genomics*, **10**(1), 334.
- Orengo, D., Puerma, E., Papaceit, M., Segarra, C., and Aguadé, M. (2015). A molecular perspective on a complex polymorphic inversion system with cytological evidence of multiply reused breakpoints. *Heredity*, **114**(6), 610–618.
- Ozer, E. A., Allen, J. P., and Hauser, A. R. (2014). Characterization of the core and accessory genomes of *Pseudomonas aeruginosa* using bioinformatic tools Spine and Agent. *BMC genomics*, **15**(1), 1.
- Pevzner, P. and Tesler, G. (2003a). Genome rearrangements in mammalian evolution: lessons from human and mouse genomes. *Genome research*, **13**(1), 37–45.
- Pevzner, P. and Tesler, G. (2003b). Human and mouse genomic sequences reveal extensive breakpoint reuse in mammalian evolution. *Proceedings of the National Academy of Sciences*, **100**(13), 7672–7677.
- Pevzner, P. and Tesler, G. (2003c). Transforming men into mice: the Nadau-Taylor chromosomal breakage model revisited. In *Proceedings of the seventh annual international conference on Research in computational molecular biology*, pages 247–256. ACM.
- Puerma, E., Orengo, D. J., Salguero, D., Papaceit, M., Segarra, C., and Aguadé, M. (2014). Characterization of the breakpoints of a polymorphic inversion complex detects strict and broad breakpoint reuse at the molecular level. *Molecular biology and evolution*, page msu177.
- Rajaraman, A., Tannier, E., and Chauve, C. (2013). Fpsac: fast phylogenetic scaffolding of ancient contigs. *Bioinformatics*, **29**(23), 2987–2994.
- Ranz, J. M., Maurin, D., Chan, Y. S., Von Grothuss, M., Hillier, L. W., Roote, J., Ashburner, M., and Bergman, C. M. (2007). Principles of genome evolution in the *Drosophila melanogaster* species group. *PLoS Biol*, **5**(6), e152.
- Samonte, R. V. and Eichler, E. E. (2002). Segmental duplications and the evolution of the primate genome. *Nature Reviews Genetics*, **3**(1), 65–72.
- Sankoff, D. (2009). The where and wherefore of evolutionary breakpoints. *Journal of biology*, **8**(7), 1.
- Sankoff, D. and Trinh, P. (2005). Chromosomal breakpoint reuse in genome sequence rearrangement. *Journal of Computational Biology*, **12**(6), 812–821.
- Tesler, G. (2002a). Efficient algorithms for multichromosomal genome rearrangements. *Journal of Computer and System Sciences*, **65**(3), 587–609.
- Tesler, G. (2002b). Grimm: genome rearrangements web server. *Bioinformatics*, **18**(3), 492–493.
- Tettelin, H., Masiagnani, V., Cieslewicz, M. J., Donati, C., Medini, D., Ward, N. L., Angiuoli, S. V., Crabtree, J., Jones, A. L., Durkin, A. S., et al. (2005). Genome analysis of multiple pathogenic isolates of *Streptococcus agalactiae*: implications for the microbial pan-genome. *Proceedings of the National Academy of Sciences of the United States of America*, **102**(39), 13950–13955.
- Thomas, A., Varré, J.-S., and Ouangraoua, A. (2011). Genome dedoubling by dcj and reversal. *BMC bioinformatics*, **12**(9), 1.